The continuum limit of quark number susceptibilities

Rajiv V. Gavai* and Sourendu Gupta†
Department of Theoretical Physics,
Tata Institute of Fundamental Research,
Homi Bhabha Road, Mumbai 400005, India.

We report the continuum limit of quark number susceptibilities in quenched QCD. Deviations from ideal gas behaviour at temperature T increase as the lattice spacing is decreased from $T/4$ to $T/6$, but a further decrease seems to have very little effect. The measured susceptibilities are 20% lower than the ideal gas values, and also 10% below the hard thermal loop (HTL) results. The off-diagonal susceptibility is several orders of magnitude smaller than the HTL results. We verify a strong correlation between the lowest screening mass and the susceptibility. We also show that the quark number susceptibilities give a reasonable account of the Wroblewski parameter, which measures the strangeness yield in a heavy-ion collision.

PACS numbers: 11.15.Ha, 12.38.Mh

I. INTRODUCTION

With the RHIC now in its second year of running, it is important to pin down lattice predictions for the high temperature phase of QCD. In this context, fully non-perturbative measurements of quark number susceptibilities [1, 2, 3, 4] are important for four reasons. Firstly, they are directly related to experimental measurements of event-to-event fluctuations in particle production [5]. Secondly, earlier results [3, 4] showed a strong jump in the susceptibility across the phase transition, but indicated a significant departure from weak-coupling behaviour, and it is important to check whether this persists into the continuum. Third, resummed perturbative computations of this quantity have now become available [6], thus making it possible to accurately test the importance of non-perturbative contributions to this quantity. Finally, with continuum extrapolated results in hand, one can address the question of whether the strangeness production seen in heavy-ion collisions can be quantitatively explained as a signal of the quark-gluon plasma.

We have recently presented systematic results for quark number susceptibilities in quenched QCD [3] as well as for QCD with two flavours of light dynamical quarks [4]. In these studies a large range of temperatures, T, was covered at a series of different quark masses, m. These computations were done at a fixed cutoff with the lattice spacing, $a = T/4$ while keeping the finite volume effects under control so that the thermodynamic limit could be taken reliably. There was a 3–5% difference between the quenched and dynamical computations. In this paper we examine the cutoff dependence of the quenched results and report their continuum (zero lattice spacing) limit.

The partition function of QCD with three quark flavours is

$$Z(T, \mu_u, \mu_d, \mu_s) = \int \mathcal{D}U \exp[-S(T)] \prod_{f=u,d,s} \det M(T, m_f, \mu_f), \tag{1}$$

where the temperature T determines the size of the Euclidean time direction, $S(T)$ is the gluonic part of the action and the determinants of the Dirac matrices, M, contain as parameters the quark masses, m_f, and the chemical potentials μ_f for each of the flavours $f = u, d, s$. We also define the chemical potentials $\mu_0 = \mu_u + \mu_d + \mu_s$, $\mu_3 = \mu_u - \mu_d$ and $\mu_8 = \mu_u + \mu_d - 2\mu_s$, which correspond to the diagonal flavour $SU(3)$ generators. Note that μ_0 is the usual baryon chemical potential and μ_3 is an isovector chemical potential.

Quark number densities are defined as

$$n_i(T, \mu_u, \mu_d, \mu_s) = \frac{T}{V} \frac{\partial \log Z}{\partial \mu_i}, \tag{2}$$

*Electronic address: gavai@tifr.res.in
†Electronic address: sgupta@tifr.res.in

and the susceptibilities as

$$\chi_{ij}(T,\mu_u,\mu_d,\mu_s) = \frac{T}{V}\frac{\partial^2 \log Z}{\partial\mu_i\partial\mu_j}, \tag{3}$$

where V denotes the spatial volume. The subscripts i and j are either of the index sets f or $\alpha = 0$, 3 and 8. We lighten the notation by writing the diagonal susceptibilities χ_{ii} as χ_i. We determine the susceptibilities at zero chemical potential, $\mu_f = 0$. In this limit, all $n_i(T) = 0$. Since we work with $m_u = m_d = m < m_s$, we also have $\chi_{03} = 0$.

Flavour off-diagonal susceptibilities such as

$$\chi_{ud} = \left(\frac{T}{V_3}\right)\left\langle \mathrm{tr}M_u^{-1}M_u'\ \mathrm{tr}M_d^{-1}M_d'\right\rangle \tag{4}$$

are given entirely in terms of the expectation values of disconnected loops. Since $m_u = m_d$, we obtain $\chi_{us} = \chi_{ds}$ with each defined by an obvious generalization of the formula above. Of the flavour diagonal susceptibilities we shall use

$$\chi_s = \left(\frac{T}{V_3}\right)\left[\left\langle\left(\mathrm{tr}M_s^{-1}M_s'\right)^2\right\rangle + \left\langle \mathrm{tr}\left(M_s^{-1}M_s'' - M_s^{-1}M_s'M_s^{-1}M_s'\right)\right\rangle\right]. \tag{5}$$

$\chi_u = \chi_d$ are given by a generalization of this formula. Numerically, the simplest quantity to evaluate is the diagonal iso-vector susceptibility

$$\chi_3 = \frac{1}{2}\left(\frac{T}{V_3}\right)\left\langle \mathrm{tr}\left(M_u^{-1}M_u'' - M_u^{-1}M_u'M_u^{-1}M_u'\right)\right\rangle. \tag{6}$$

Two more susceptibilities are of interest. These are the baryon number and electric charge susceptibilities,

$$\chi_0 = \frac{1}{9}\left(4\chi_3 + \chi_s + 4\chi_{ud} + 4\chi_{us}\right) \qquad \text{and} \qquad \chi_q = \frac{1}{9}\left(10\chi_3 + \chi_s + \chi_{ud} - 2\chi_{us}\right). \tag{7}$$

Note that χ_0 is the baryon number susceptibility for three flavours of quarks. As a result, this expression differs from the iso-singlet quark number susceptibility for two flavours, defined in [1], both in overall normalization and by terms containing strangeness. In our numerical work we have chosen to use staggered quarks. Hence, to normalise to one flavour of continuum quarks and compensate for fermion doubling on the lattice, we have to multiply each of the traces in eqs. (4–6) by a factor of 1/4.

The quark mass appears in two logically distinct places— first in the operators which define the susceptibilities in eqs. (4–6), and secondly in the determinant in the partition function of eq. (1) which defines the weight for the averaging of these operators. The first defines a valence quark mass and the second the sea quark mass. In this paper we adopt the quenched approximation, whereby the determinants in eq. (1) are set equal to unity. However, we shall vary the valence quark masses. As shown earlier, unquenching the sea quarks changes results by 3–5% [3, 4].

Note that all the flavour off-diagonal susceptibilities are exactly zero in an ideal gas. We shall denote by χ^3_{FFT} the ideal gas value for χ_3. On an $N_t \times N_s^3$ lattice with N_c colours and lattice spacing a, we find

$$a^2\chi^3_{FFT} = \frac{N_c}{2N_tN_s^3}\sum_p\left\{D^{-2}\sin^2 p_0\cos^2 p_0 + D^{-1}\left(\sin^2 p_0 - \frac{1}{2}\right)\right\}, \tag{8}$$

where the spectrum of momenta is $p_0 = (2\pi/N_t)(n+1/2)$ with $0 \le n < N_t$ and $p_i = 2\pi n/N_s$ with $0 \le n < N_s$, and $D = (ma)^2 + \sum_\mu \sin^2 p_\mu$. For a given m/T_c and T/T_c, the value of the quark mass in lattice units is

$$ma = \left(\frac{1}{N_t}\right)\left(\frac{m}{T_c}\right)\left(\frac{T_c}{T}\right). \tag{9}$$

The formula in eq. (8) is normalised such that there is exactly one copy of each flavour of quarks. The values of χ_s, χ_0 and χ_q for an ideal gas can then be simply obtained as linear combinations of χ^3_{FFT} for different valence quark masses.

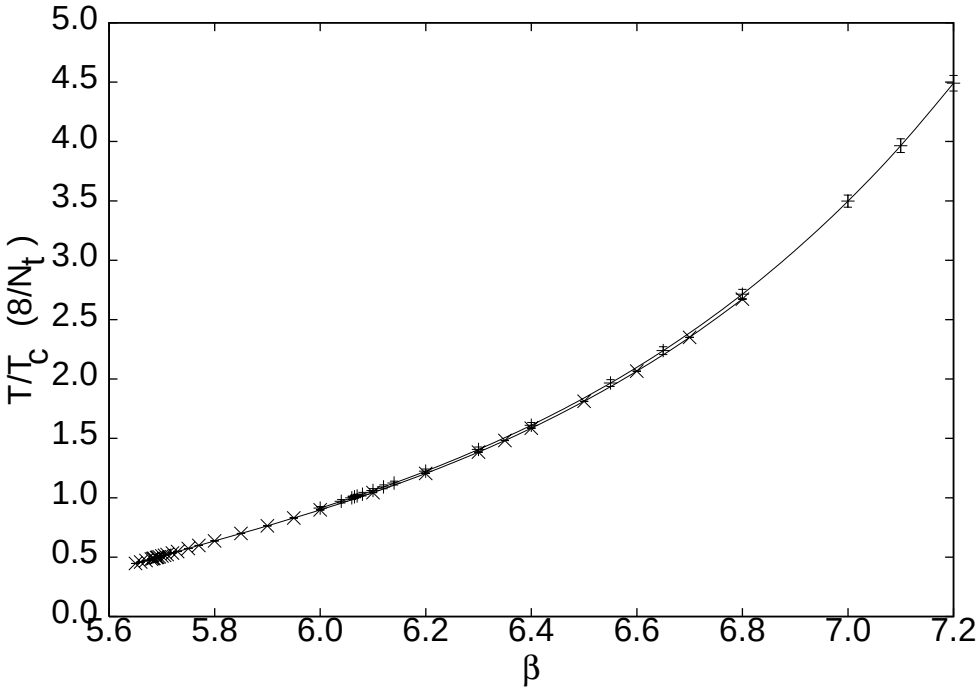

FIG. 1: The temperature for any value of N_t for a given coupling β. Crosses denote data for $N_t = 4$ lattices and pluses for $N_t = 8$ lattices. The scale has been set by a corrected QCD 2-loop formula [9]. The difference between the two sets of data is a measure of scale breaking by residual power-law corrections and is negligible within statistical errors.

II. LATTICE RESULTS

We have previously reported measurements of χ_3 in quenched QCD with 4 time slices ($N_t = 4$) at temperatures of $1.1T_c$, $1.25T_c$, $1.5T_c$, $2T_c$ and $3T_c$ [2]. We have extended these measurements to higher temperatures through two simulations on 4×20^3 lattices at $\beta = 6.6$ and 6.7. These correspond to temperatures of $4.13T_c$ and $4.7T_c$. All these computations are performed at fixed bare quark masses of $m/T_c = 0.03$, 0.3, 0.5, 0.75 and 1 (the data for $m/T_c = 0.5$ are new).

The continuum limit has been taken by going to several smaller lattice spacings. One set of computations is performed with a lattice spacing $a = 1/6T$ which is 33% smaller than the lattice spacing used earlier. We have taken data on 6×20^3 lattices at $\beta = 6.0625$, 6.3384 and 6.7 corresponding to $T/T_c = 1.333$, 2 and 3.133, and on a 6×24^3 lattice at $\beta = 6.8$ corresponding to $T/T_c = 3.532$. One further computation was made on an 8×18^3 lattice at $\beta = 6.55$. This corresponds to $T/T_c = 2$ with lattice spacing $a = 1/8T$. The quark mass m/T_c is kept independent of a and T, and hence ma decreases with increasing T at fixed N_t or with increasing N_t at fixed T according to eq. (9).

The lattice scale has been set using the plaquette measurements of [8] and the analysis performed in [9]. The conversion of β to T using data for $N_t = 4$ and 8 give the two curves in Figure 1. The difference between the two curves is within the statistical uncertainty of 5% on the scale assignment. There is the same degree of statistical uncertainty in the bare quark masses and in all other scales. We shall not display this inherent scale uncertainty in the measurements, but it should be kept in mind.

The simulations have been performed with a Cabbibo-Marinari pseudo-heatbath technique with 3 $SU(2)$ subgroups updated on each hit. An initial 1000 sweeps have been discarded for thermalisation. On the $N_t \leq 6$ lattices we have used 80 configurations separated by 1000 sweeps for the measurements. On the $N_t = 8$ lattice we have used 55 configurations separated by 500 sweeps.

We have previously checked that the spatial lattice size, $L = N_s a$, is quite irrelevant to the values of χ measured as long as it is sufficiently large compared to the inverse pion mass [2, 4]. In fact, at all the couplings and quark masses we have used, $m_\pi L \geq 5$. The most important other constraint on L comes from the requirement that it should be large enough to prevent spatial deconfinement [7]. This is ensured by taking $N_s/N_t \geq T/T_c$ in all our simulations.

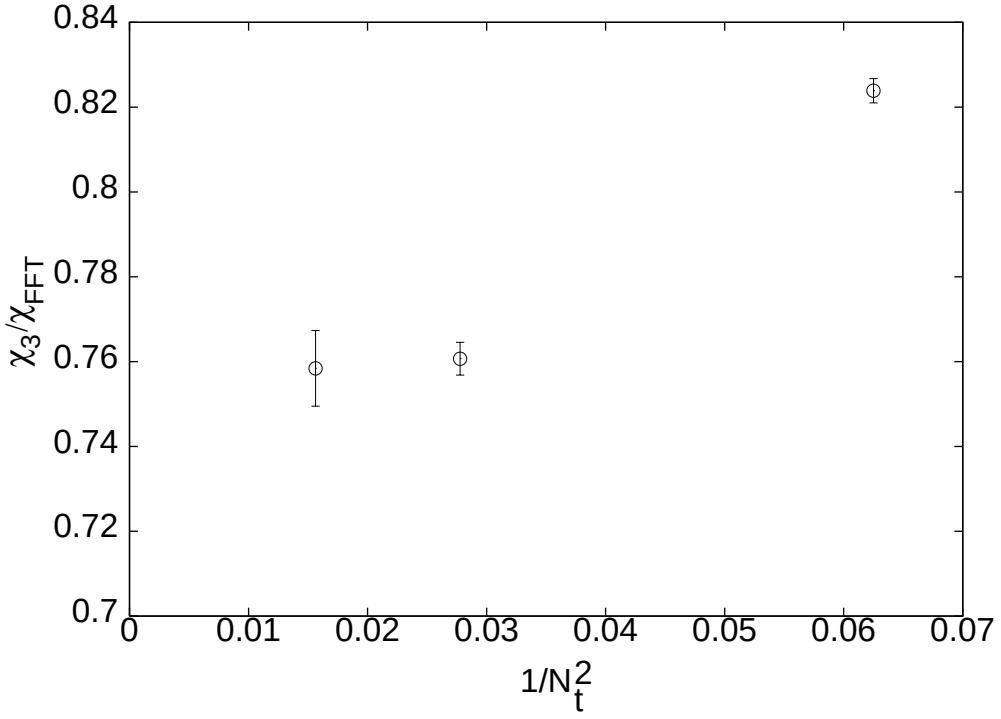

FIG. 2: χ_3/χ^3_{FFT} at $T = 2T_c$ shown as a function of $a^2 \propto 1/N_t^2$ for $m/T_c = 0.03$. The ratio reaches its continuum limit when evaluated on lattices with $N_t = 6$.

The traces are evaluated by the usual stochastic technique,

$$\mathrm{Tr}\, A = \frac{1}{2N} \sum_{i=i}^{N} R_i^\dagger A R_i, \tag{10}$$

where R_i are a set of N uncorrelated vectors with components drawn independently from a Gaussian ensemble with unit variance. Each vector has three colour components at each site of the lattice. Since we use a half lattice version of the Dirac operator for staggered Fermions, the number of components of each vector R_i is one and a half times the number of lattice points. $(\mathrm{Tr}\, A)^2$ is obtained by dividing the set of R_i into disjoint blocks, constructing $\mathrm{Tr}\, A$ in each block, taking all possible distinct pairs of such estimates, multiplying them and then averaging over the pairs. For $N_t = 4$ it is possible to get accurate results with $N \approx 10$, although we have chosen to use $N = 80$ for each gauge configuration [4].

It is easy to check that the variance of the estimator above is proportional to $\mathrm{Tr}(A^2)$. Since the diagonal element of the Fermion matrix is proportional to the quark mass ma, whereas the off-diagonal elements are bounded by unity, with increasing T or decreasing a, $\mathrm{Tr}\, A$ decreases linearly, while its variance remains constant. Hence, for sufficiently small ma the number of vectors has to increase quadratically with ma. We found that $N_v = 100$ was sufficient for $N_t = 8$ at $T = 2T_c$, although at larger N_t or T significantly larger values of N_v are needed. A further numerical problem arises from the cancellation of the two matrix elements which give χ_3 (see eq. 6). While increasing N_t and keeping the physical size of the lattice fixed, each of these terms increases quadratically but mutually cancel to give a number which decreases quadratically with N_t. At fixed word length, this implies a reduction in accuracy by a factor of N_t^4.

In Figure 2 we show how the continuum limit of χ_3 is reached. There is an 8% decrease in χ_3/χ^3_{FFT} in going from $N_t = 4$ to $N_t = 6$ lattices. However, within measurement errors, the continuum limit is reached already at $N_t = 6$. This implies a cancellation of the N_t-dependence of χ_3 and χ^3_{FFT}. The reason for the atypical behaviour for $N_t = 4$ is not in the numerator, which is non-perturbative, but in the denominator, which is the ideal gas.

For $N_t = 4$, the spectrum of p_0 consists of $\{\pm\pi/4, \pm 3\pi/4\}$. As a result, $\sin^2 p_0 = 1/2$ and the second term in the sum on the right of eq. (8) vanishes identically. This accident occurs only for $N_t = 4$, and for all other values of N_t this term contributes a non-vanishing value. It is easy to see that in the limit $N_t \to \infty$ this term contributes to the leading part of χ^3_{FFT}. This is the reason the values for χ_3/χ^3_{FFT} for $N_t = 4$ lie well away from the continuum limit.

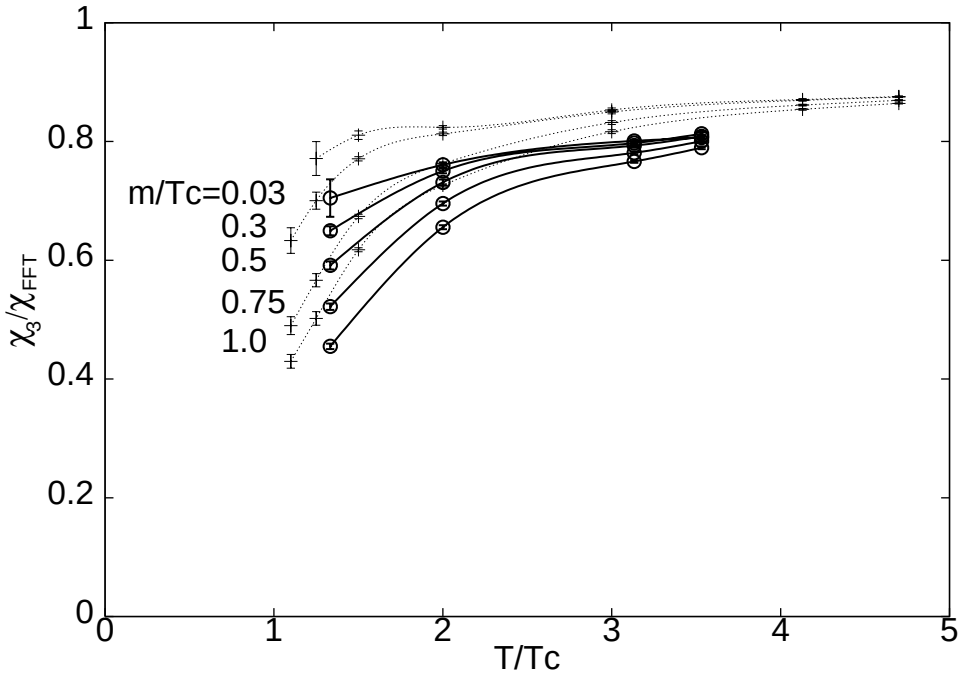

FIG. 3: The ratio χ_3/χ^3_{FFT} in quenched QCD, shown as a function of T for the values of m/T_c indicated. Pluses denote data for lattice spacing $a = 1/4T$ and circles for $a = 1/6T$. The lines are cubic spline fits to the data.

T/T_c	χ_3/χ^3_{FFT}	χ_{ud}/T^2	χ_s/χ^s_{FFT}	χ_0/χ^0_{FFT}	χ_q/χ^q_{FFT}
1.333	0.70 (3)	$(2 \pm 4) \times 10^{-6}$	0.455 (5)	0.66 (2)	0.68 (3)
2.000	0.761 (3)	$(-1 \pm 2) \times 10^{-7}$	0.656 (3)	0.740 (3)	0.751 (3)
3.133	0.801 (2)	$(-1 \pm 1) \times 10^{-7}$	0.766 (2)	0.794 (2)	0.798 (2)
3.532	0.807 (2)	$(1 \pm 2) \times 10^{-7}$	0.789 (2)	0.803 (2)	0.805 (2)

TABLE I: Results for the continuum limit of quark number susceptibility in quenched QCD. We have taken $m_s/T_c = 1$ as appropriate to full QCD. Our $N_t = 4$ results indicate that at higher T the ratios χ/χ_{FFT} remain flat.

Our complete results for the dependence of χ_3/χ^3_{FFT} on T/T_c at several different quark masses for $N_t = 4$ and 6 are shown in Figure 3. In view of the data shown in Figure 2, our results for $N_t = 6$ are the continuum limit for the quenched theory: these are summarised in Table I. Note that even at temperature as high as $3.5T_c$ the result is far below the ideal gas limit. Closer to T_c there is an even more dramatic fall in the value of χ_3/χ^3_{FFT}. We have also measured the off-diagonal susceptibility χ_{ud}. As already seen for $N_t = 4$ this is consistent with zero. In Table I we show that the continuum limit of χ_{ud} also vanishes within errors of $10^{-7}T^2$. It is therefore much smaller than the 3-loop perturbative result given in [6].

Note that the continuum limit of our measurements lie 20–30% below the ideal gas result. They also differ significantly from HTL as well as the skeleton graph resummed results of [6]. At $T = 3T_c$, HTL predicts $\chi_3/\chi^3_{FFT} = 0.90$–$0.94$ on varying the scale of α_s between πT and $4\pi T$, and the resummed computation gives $\chi_3/\chi^3_{FFT} = 0.95$–$0.97$. Our measurement shows $\chi_3/\chi^3_{FFT} = 0.80$ at $3T_c$ (see Table I). A second computation of the HTL result is available for $N_f = 2$ [10]. Since this agrees with the HTL result of [6] for $N_f = 2$, we believe the HTL result for χ_3/χ^3_{FFT} is under control. There is thus a genuine discrepancy between these lattice results and existing perturbative computations.

The quark number susceptibilities are closely related to the screening correlator of a one-link separated quark bilinear operator which corresponds to a ρ meson at zero temperature. The $T > 0$ transfer matrix of the problem mixes this with a quark bilinear that corresponds to the π [11]. We have earlier shown evidence for $N_t = 4$ that χ_3 is closely related to the only known non-perturbative quantity among the screening correlators, that is the screening mass M_S coming from the two degenerate correlators that descend from the π and σ operators of the zero temperature theory [4]. In view of the strongly non-perturbative character of χ_3, as revealed by the comparison with HTL and

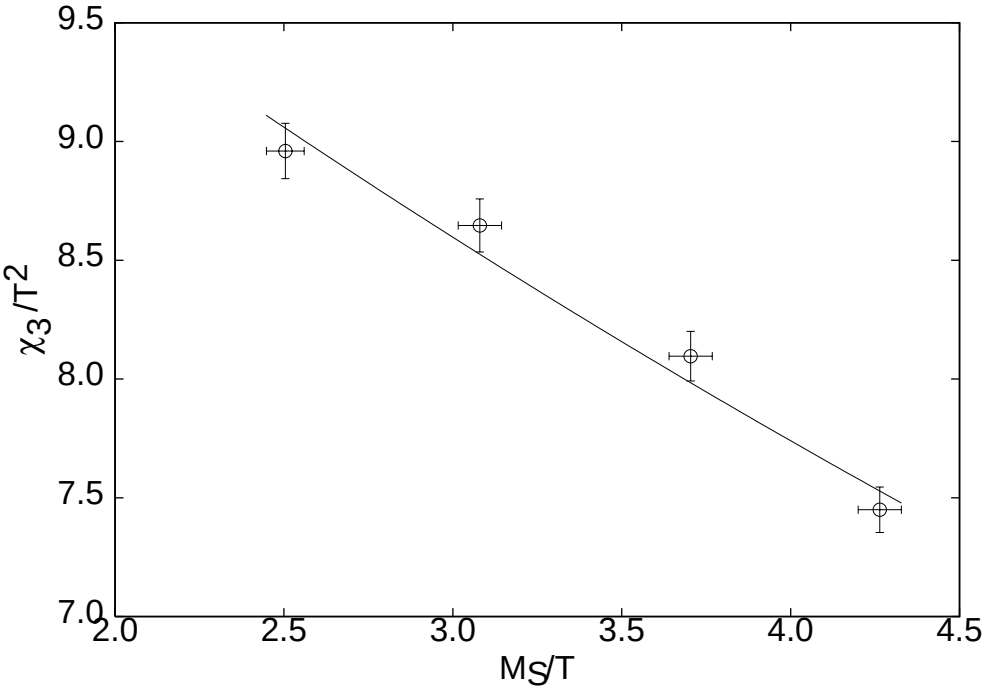

FIG. 4: Correlation between the screening mass in the scalar/pseudo-scalar sector, M_S, and the quark number susceptibility, χ_3 at $2T_c$. The measurements have been made on a 8×18^3 lattice at a series of quark masses. The line is an exponential fit to the data.

resummation explained above, examining this correlation in the continuum becomes more significant. In Figure 4 we show data obtained on 8×18^3 lattices which indicate that this correlation survives into the continuum.

III. STRANGENESS

Measurements of hadron yields in relativistic heavy-ion collisions have been analysed extensively [12, 13] and the observed enhancement of strangeness has been claimed to be evidence for quark-gluon plasma formation. The chemical composition is observed at the hadron freezeout temperature, which has been found to be very close to the value of T_c in full QCD. It has been argued that this chemical composition cannot arise due to hadronic rescattering [14]. It would be interesting if it could be directly determined whether or not the composition is characteristic of the plasma for $T \geq T_c$. We argue below that this question can be answered by a lattice QCD measurement such as we have presented above.

The quantity which seems to be directly connected to lattice measurements is the Wroblewski parameter [15], λ_s, which measures the ratio of newly created primary strange to light quarks—

$$\lambda_s = \frac{2\langle s\bar{s}\rangle}{\langle u\bar{u} + d\bar{d}\rangle}. \tag{11}$$

A fluctuation-dissipation theorem relates the rate of production of quark pairs by the plasma in equilibrium to the imaginary part of the full complex quark number susceptibilities [16]. If the inverse of the characteristic time scales of the QCD plasma are not close to the typical energy scales for the production of strange and lighter quarks, then the ratio of their production rates is just the ratio of the static susceptibilities that we have measured. Then, if the observed chemical composition is created in equilibrium, we should have

$$\lambda_s = \frac{2\chi_s}{\chi_u + \chi_d} \approx \frac{\chi_s}{\chi_u}, \tag{12}$$

where the last equality holds in the limit of equal u and d quark masses. These susceptibilities have to be evaluated on the lattice at the temperature and chemical potential, μ_0, relevant to the collision. However, it has been shown

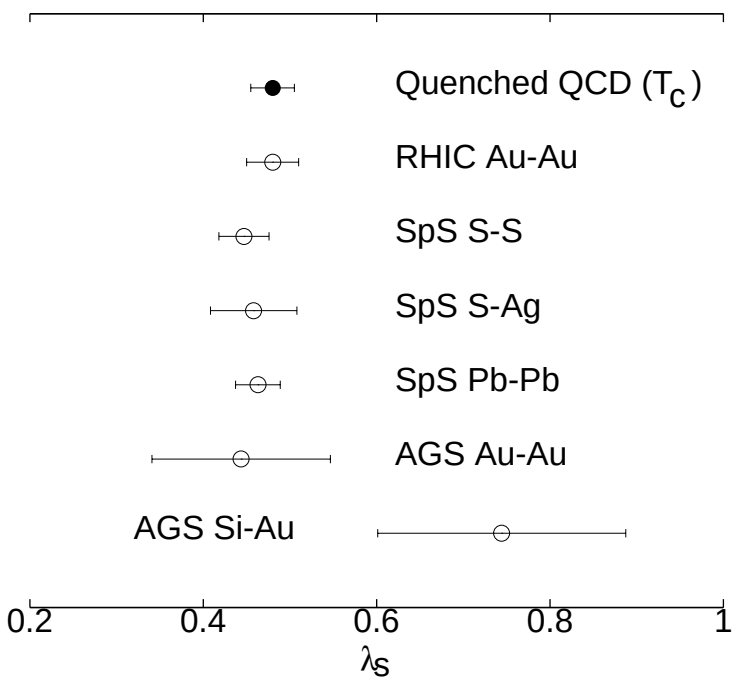

FIG. 5: The Wroblewski parameter, λ_s, obtained from various experimental measurements, compared with the value obtained from the lattice measurements reported here.

recently [17] that λ_s is insensitive to μ_0 for SpS and RHIC energies. Furthermore a lattice measurement shows that the screening mass, M_S, does not change rapidly with increasing chemical potential [18]. Then, in view of the correlation between M_S and χ shown in Figure 4, we do not expect rapid changes with chemical potential in the ratio above. Both these arguments show that as a first approximation one can take the ratio in eq. (12) at zero chemical potential.

From our measurements of χ reported here, we can form the lattice "prediction" of λ_s created in the plasma at T_c. This has been done by taking our measurements at $T/T_c = 4/3$ and 2, and extrapolating them linearly to T_c. For χ_u we use data taken for $m/T_c = 0.03$, which is light enough for this purpose. Since scaled quantities feel the smallest correction for unquenching [4], we take χ_s to correspond to $m/T_c = 1$, which is appropriate to full QCD. In Figure 5 the resultant prediction is compared with the data collected in [13, 17]. It can be seen that there is a fair agreement with the data. However, this is subject to several assumptions—

1. The foremost assumption is that the characteristic time scales of the plasma are not close to the inverse energy scale of the production processes. It is not possible to test this assumption in an Euclidean computation. However, it has been suggested that these characteristic time scales could be observed in real or virtual photon production as spikes in the spectrum [19]. If these are seen and they lie in the energy range for the production, the assumption would be falsified.

2. Another important assumption is that chemical equilibration takes place in the plasma. If chemical equilibrium is not achieved but the light degrees of freedom achieve energy equipartition, then the effective temperature could be higher.

3. We have assumed slow variation of the ratio χ_s/χ_u with chemical potential. While this seems to be a reasonable estimate in view of the results of [17, 18] and our own observations about the relation between the lowest screening mass and the susceptibilities, one should keep in mind possible changes in the ratio due to violation of this assumption.

4. Our continuum results are obtained in quenched QCD, whereas the data corresponds to full QCD. As mentioned already, we have taken $m/T_c = 1$, as appropriate to full QCD, in order to correct for this. However, an additional 5–10% shift in our results could arise when unquenching [4]. This is not shown in Figure 5.

5. Our measurements are made away from T_c and extrapolated down to this temperature. In principle this can be corrected by a computation made directly at T_c. However, due to the enormous cost of extracting physical quantities at T_c, we postpone this to the time when we attempt a full QCD simulation.

It might seem surprising that λ_s corresponds to the chemical composition at T_c. However, a moment's thought shows that this is entirely in accord with the assumption of chemical equilibrium. Even if the system is thermalized at a much higher temperature, it remains in equilibrium until it reaches T_c. Departure from equilibrium as the system cools through the transition is unlikely, and if it occurs, should have a visible signature such as the formation of a disoriented chiral condensate [20]. In the absence of such phenomena, if λ_s does not correspond to the chemistry at T_c, then the second assumption above would be demonstrated to be false. Also, with increasing ion energy the system moves closer to zero baryon number, as seen at RHIC. This makes our third assumption better at the RHIC and LHC. The fourth assumption can be removed by a computation with full QCD. Such a computation is planned, where also the final assumption can be removed, and will be reported elsewhere.

IV. SUMMARY

In summary, we have presented new and precise results on quark number susceptibilities over a wide range of temperatures and quark masses in the high temperature phase of QCD. The main aim of this study was to obtain the continuum extrapolation of these susceptibilities. As shown in Figure 2, while there is a significant change in going from $N_t = 4$ to $N_t = 6$ lattices, there is no statistically significant change in the susceptibilities beyond this. The results obtained for $N_t = 6$ lattices can then be taken as the continuum limit. This limit is shown in Figure 3 and Table I.

There is a strong discrepancy between the continuum extrapolated lattice results and HTL computations for these quantities— varying between about 12% at the highest T to even larger at smaller T. The off-diagonal susceptibility, χ_{ud}, is zero, in contrast to the HTL results. There is a somewhat larger discrepancy between the continuum extrapolated lattice results and the skeleton graph resummed results. The conjecture that there is a strong non-perturbative component to the quark number susceptibilities is supported by an observed strong correlation between the smallest quark bilinear screening mass, M_S, and the susceptibility χ_3 (Figure 4).

It is interesting to note that the continuum extrapolated results for the strange and light quark susceptibilities can be used to give a surprisingly good description of the chemical composition of hadrons at freezeout in SpS and RHIC experiments (Figure 5). This has to be treated as a preliminary estimate due to the many caveats which we have listed, and some of which we plan to check in future lattice measurements.

[1] S. Gottlieb *et al.*, *Phys. Rev. Lett.* 59 (1987) 2247.
[2] R. V. Gavai *et al.*, *Phys. Rev.* D 40 (1989) 2743;
C. Bernard *et al.*, *Phys. Rev.* D 54 (1996) 4585;
S. Gottlieb *et al.*, *Phys. Rev.*, D 55 (1997) 6852.
[3] R. V. Gavai and S. Gupta, *Phys. Rev.* D 64 (2001) 074506.
[4] R. V. Gavai, S. Gupta and P. Majumdar, hep-lat/0110032, *Phys. Rev.* D, in press.
[5] M. Asakawa, U. Heinz and B. Müller, *Phys. Rev. Lett.* 85 (2000) 2072;
S. Jeon and V. Koch, *ibid.* 85 (2000) 2076;
D. Bower and S. Gavin, *Phys. Rev.* C 64 (2001) 051902;
S. Jeon, V. Koch, K. Redlich and X. N. Wang, nucl-th/0105035.
[6] J.-P. Blaizot, E. Iancu and A. Rebhan, hep-ph/0110369.
[7] S. Datta and S. Gupta, *Phys. Lett.*, B 471 (2000) 382.
[8] G. Boyd *et al.*, *Nucl. Phys.*, B 469 (1996) 419.
[9] S. Gupta, *Phys. Rev.*, D 64 (2001) 034507.
[10] P. Chakraborty, M. G. Mustafa and M. H. Thoma, hep-ph/0111022, to appear in *Euro. Phys. J.* C.
[11] S. Gupta, *Phys. Rev.*, D 60 (1999) 094505.
[12] P. Braun-Munzinger *et al.*, *Phys. Lett.*, B 465 (1999) 43;
J. Letessier and J. Rafelski, *Nucl. Phys.*, A 661 (1999) 97c.
[13] F. Becattini *et al.*, *Phys. Rev.* C 64 (2001) 024901.
[14] U. Heinz *J. Phys.* G 25 (1999) 263;
R. Stock, *Phys. Lett.* B 456 (1999) 277.
[15] A. Wroblewski, *Acta Phys. Pol.*, B 16 (1985) 379.
[16] P. C. Martin, in *Many Body Physics*, Proceedings of the 1967 Les Houches School, Eds. C. DeWitt and R. Balian, Gordon and Breach, New York, 1968;

W. Marshall and S. W. Lovesey, *Theory of Thermal Neutron Scattering*, Oxford University Press, London, 1971;
A. L. Fetter and J. D. Walecka, *Quantum Theory of Many-particle Systems*, McGraw-Hill, New York, 1971.
[17] J. Cleymans, e-print hep-ph/0201142.
[18] S. Choe *et al.*, e-print hep-lat/0110223.
[19] H. A. Weldon, *Nucl. Phys.* A 525 (1991) 405c;
S. Gupta, *Nucl. Phys.* A 566 (1994) 69c.
[20] K. Rajagopal and F. Wilczek, *Nucl. Phys.*, B 404 (1993) 577.